Journal of Pharmaceutical and Biomedical Analysis 53 (2010) 359–365

Contents lists available at ScienceDirect

Journal of Pharmaceutical and Biomedical Analysis

journal homepage: www.elsevier.com/locate/jpba

In situ formation of nanoparticles upon dispersion of melt extrudate formulations in aqueous medium assessed by asymmetrical flow field-flow fractionation

Johanna Kanzer[a,b], Stefan Hupfeld[a], Terje Vasskog[c], Ingunn Tho[a], Peter Hölig[d], Markus Mägerlein[d], Gert Fricker[b], Martin Brandl[a,e,*]

[a] Drug Transport and Delivery Group, Department of Pharmacy, University of Tromsø, N-9037 Tromsø, Norway
[b] Department of Pharmaceutical Technology and Biopharmacy, Institute of Pharmacy and Molecular Biotechnology, University of Heidelberg, D-69120 Heidelberg, Germany
[c] Research Group for Natural Products and Medicinal Chemistry, Institute of Pharmacy, University of Tromsø, N-9037 Tromsø, Norway
[d] SOLIQS, Abbott GmbH and Co. KG, D-67061 Ludwigshafen, Germany
[e] Department of Physics and Chemistry, University of Southern Denmark, DK-5230 Odense M, Denmark

ARTICLE INFO

Article history:
Received 4 February 2010
Received in revised form 31 March 2010
Accepted 8 April 2010
Available online 24 April 2010

Keywords:
Solid dispersion
Melt extrudate
Asymmetrical flow field-flow fractionation
Nanoparticle
Particle size

ABSTRACT

In recent years melt extrudates (e.g. Meltrex®) have proven to be a promising formulation tool for poorly water-soluble and poorly bioavailable drugs. During the hot-melt extrusion process solid dispersions are formed. For several of these formulations improved bioavailabilities have been reported; the mechanism behind, however is still not very well understood. The aim of this study was to investigate whether solid dispersions prepared by melt extrusion upon dispersion in aqueous medium form particles and/or supramolecular assemblies. The formulation investigated here contained the human immunodeficiency virus (HIV) protease inhibitors lopinavir and ritonavir, polyvinylpyrrolidone–vinyl acetate copolymer (Kollidon® VA64), sorbitan monolaurate (Span® 20) and hydrophilic fumed silica (Aerosil® 200). The aqueous dispersions originating from both, API-containing and placebo formulation were investigated using photon correlation spectroscopy (PCS) and asymmetrical flow field-flow fractionation (AsFlFFF) with subsequent online multi-angle light-scattering (MALS) particle size analysis. The content of both APIs in the AsFlFFF-fractions was quantified using high performance liquid chromatography–mass spectrometry.

PCS indicated sub-micron particles. AsFlFFF revealed the co-existence of up to three different types of colloidal to nanoparticulate assemblies in the aqueous dispersions. Even though a complete resolution of the composition of the sub-fractions could not be achieved, the following types could be clearly distinguished: The first fraction eluting from AsFlFFF, appears to be colloidal polymer. Only marginal amounts of the APIs were found associated with the polymer. Secondly, API-rich nanoparticles eluted. Thirdly, nanoparticulate assemblies assigned to sorbitan monolaurate and/or hydrophilic fumed silica were identified. A limited amount of drug was found associated with this fraction. Using AsFlFFF–MALS the size of particles in fractions could be determined.

From this experience AsFlFFF is regarded as promising technique for investigation of particles/structures originating during dispersion of melt extrudates in aqueous medium in terms of size and type of nanoparticles and their API-content.

1. Introduction

The oral route is the major route of drug administration due to its convenience, good patient compliance and low production cost. A prerequisite for a clinical effect after permeation across the intestinal barrier into the systemic circulation is dissolution of the drug in the gastric fluid within the given time frame of passage through the gastrointestinal tract. Many new drug candidates lack sufficient (water-) solubility due to pronounced lipophilic properties. During high-throughput lead optimization screening, which is not dependent that much on solubility anymore, the in vitro activity of potential drug candidates is emphasized. In general, lipophilic groups in receptor pockets improve the potency of drugs and thus, larger and more lipophilic potential new drug candidates are more readily detectable during screening [1]. In recent years, an increasing fraction of new chemical entities (NCEs) is seen, where dissolution represents the rate-controlling step and limits the rate and degree of absorption.

* Corresponding author at: Department of Physics and Chemistry, University of Southern Denmark, Campusvej 55, DK-5230 Odense M, Denmark.
Tel.: +45 6550 2525; fax: +45 6615 8760.
E-mail address: mmb@ifk.sdu.dk (M. Brandl).

0731-7085/$ – see front matter © 2010 Elsevier B.V. All rights reserved.
doi:10.1016/j.jpba.2010.04.012

Solid dispersions are defined as dispersion of at least one active ingredient in a carrier and can be classified into eutectic mixtures, solid solutions, glassy solutions and suspensions, amorphous precipitations in a crystalline carrier and complex formations. Furthermore, combinations of the aforementioned forms and miscellaneous mechanisms are possible [2]. Several techniques for manufacturing of solid dispersions like solvent evaporation and melting method have been described in the literature. Furthermore, technologies like supercritical fluid and cryogenic freezing have been discussed recently [3]. In terms of melting methods hot-melt extrusion shows to be an efficient technique for production. Briefly, the process of melt extrusion can be divided into four steps. First, the raw material is fed to the extruder. Afterwards the mass is conveyed and enters into the die, followed by flow through the die. The last step consists of exit from the die and downstream processing. Under ideal circumstances the process results in a true molecular solution of the active agent in the matrix [4]. Solid dispersions produced by melt extrusion are of great interest regarding commercial products. One of the products on the market is Kaletra® tablets containing the human immunodeficiency virus (HIV) protease inhibitor (PIs) combination of lopinavir and ritonavir. Based on Lipinski's "rule of 5" both drugs are designated to be poorly water soluble [1]. Ritonavir has been classified as BCS class 4 drug [5]. Like other PIs lopinavir administered alone would not lead to sufficient bioavailability due to high metabolism of cytochrome P-450 3A. Co-administration of ritonavir inhibits the metabolizing enzyme and thus enhances the amount of available lopinavir in the systemic circulation [6]. Therefore, combination with ritonavir leads to improved bioavailability of lopinavir [7].

In comparison with the previously approved soft gelatine capsules the melt extrudate formulation shows less pharmacokinetic variability and diminished food effect. Furthermore, refrigerated storage is not required any more [8]. Methods for characterization of solid dispersions in its solid form are widely described in the literature and include thermodynamic techniques, X-ray diffraction and infrared spectroscopy [9]. Potential mechanisms of drug release are discussed to some extent in the literature [10–12]. In a recent study it was demonstrated that ritonavir containing melt extrudates form nano- to microparticulate dispersions in contact with aqueous medium [13].

The purpose of this study was to characterize structures/particles formed after solid dispersions prepared by melt extrusion dispersed in aqueous media with respect to size and composition. The formulations contained the HIV protease inhibitors ritonavir and lopinavir, polyvinylpyrrolidone–vinyl acetate copolymer (PVP/VA) as hydrophilic carrier, sorbitan monolaurate as non-ionic lipophilic surfactant and hydrophilic fumed silica. First, experiments regarding particle size using photon correlation spectroscopy (PSC) were performed. Furthermore, asymmetrical flow field-flow fractionation (AsFlFFF) coupled to online multi-angle light scattering (MALS) was employed for fractionation of particles arising from aqueous dispersions of melt extrudates according to size and for determination of size distribution. The content of drug in fractions collected with AsFlFFF was analysed using high performance liquid chromatography–mass spectrometry (HPLC–MS/MS).

AsFlFFF–MALS is part of a family of versatile fractionation techniques capable of performing separation and simultaneously particle size determination. In brief, particles/structures are separated according to their size/hydrodynamic radius due to different diffusion coefficient in a parabolic laminar field, which results from a carrier liquid pumped through the narrow ribbon channel. The equilibrium height of different sized particles above the accumulation wall is determined by the cross flow applied perpendicular to the channel flow and the Brownian motion of the particles. Smaller particles with higher diffusion coefficients are positioned at levels in the channel more distant from the accumulation wall. Therefore, these particles elute faster than larger analytes, which are positioned near to the accumulation wall (Fig. 1) [14,15]. Estimation of the particle size can be performed based on the different diffusion coefficients applying Stokes law. In order to calculate the size of eluting particles it is advantageous to couple the AsFlFFF system to a MALS detector. Determination of size with MALS is based on the measurement of the intensity of scattered light at different angles around a particle. From the intensity of the scattered light the molar mass and the radius of particle can be calculated as described in the literature [16].

2. Materials and method

2.1. Materials

Sodium nitrate, acetonitrile (LiChrosolv®) and formic acid were purchased from Merck, KGaA, Germany. D_3-testosterone was obtained from Toronto Research Chemicals, North York, Canada. Polyvinylpyrrolidone–vinyl acetate copolymer (PVP/VA) (Kollidon® VA64) and two formulations (Table 1), prepared by melt extrusion, were provided by SOLIQS, Abbott GmbH & Co. KG, Ludwigshafen, Germany. Sorbitan monolaurate (Span® 20) with an HLB value of 7.6–9.6 was employed as surfactant. For preparation of solutions for AsFlFFF, ultrapure water from a Milli-Q® Academic system (Millipore Corporation, Billerica, USA) was used.

2.2. Methods

2.2.1. Melt extrusion

Preparation of the solid dispersions was performed by hot-melt extrusion according to the Meltrex technology as described in [4]. In brief: a blend of raw materials was introduced into a con-rotating twin-screw extruder at temperature ranges of 100–150 °C. The melt was directly calendered after extrusion and solid oblong shaped tablets of extruded material were obtained.

2.2.2. Wide angle X-ray scattering

The extrudate was investigated for crystalline parts of lopinavir and ritonavir using wide angle X-ray scattering (WAXS). Powder X-ray diffraction patterns were recorded using a Panalytical X'Pert Pro MPD diffractometer (Panalytical, Almelo, The Netherlands) with a Pixcel detector, Data Collector and High Score software. Measurements were performed with a Cu Kα radiation source at 40 kV voltage and 40 mA current from 5° to 27° 2-theta in a continuous scanning mode. The instrument was set to a step width of 0.026° 2-theta and a measurement time per step of 4000 s. The irradiated sample length was 20 mm. Sample preparation was done by milling approximately 1.5 g of extrudate with a ball mill (Pulverisette 23, Fritsch, Idar-Oberstein, Germany) at 50 Hz for 20 s. A backloading 27 mm diameter powder diffraction sample holder (Panalytical) was used for the measurements.

2.2.3. Sample preparation

Sample dispersions were prepared dispersing a piece of melt extrudate in sodium nitrate solution (10 mM, pH ~ 5.5) by magnetic stirring for 1 h at 400 rpm, 37 °C. A constant stirring rate and a temperature equal the temperature in the human body reflected a standardized procedure. The final concentrations relating to the amount of the extrudates corresponded to 0.8 mg/ml ritonavir and 3.2 mg/ml lopinavir. The concentrations were chosen related to pharmacological relevant concentrations. For the analysis of placebo extrudate and PVP/VA solution with a concentration of surfactant and polymer, respectively, related to the concentration of associated extrudate with API was prepared. 10 mM sodium nitrate solution as carrier liquid and dispersion medium

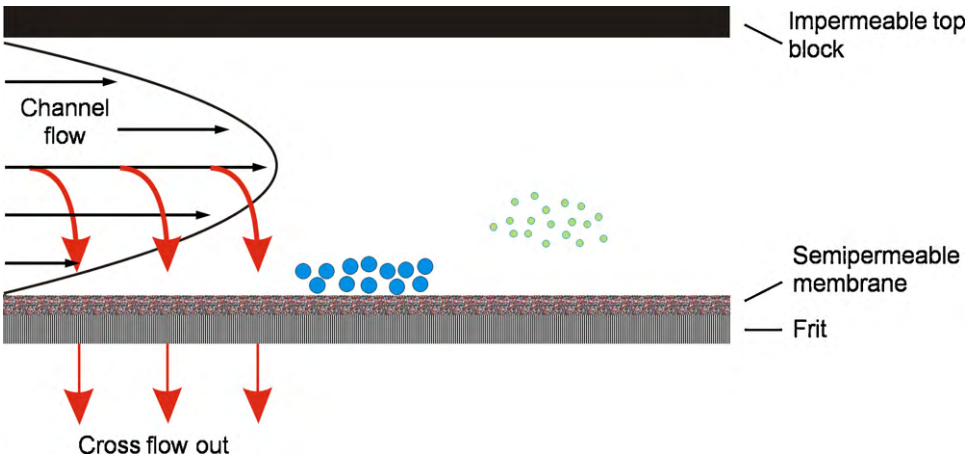

Fig. 1. Cross-section through an AsFlFFF channel.

was freshly prepared and the solution was filtered through a membrane with a pore size of 0.1 μm (Vacucap 90 filter unit with 0.1 μm supor® membrane, Pall Life Sciences, Ann Arbor, MI, USA) for AsFlFFF- and 0.22 μm (Bottle Top Filter with 0.22 μm polystyrene membrane, Corning, Schiphol, The Netherlands) for PCS-analysis. During AsFlFFF experiments sodium nitrate solution was used as an established carrier liquid. Primarily ionic strength but also the composition of the carrier liquid had shown to influence the elution process. Moderate ionic strength has been investigated regarding its effect on the elution behaviour of various nanoparticles and a concentration of 10 mM sodium nitrate was recommended [17–20]. To avoid effects of different ionic strengths 10 mM sodium nitrate was also employed as dispersion medium.

2.2.4. Photon correlation spectroscopy

The PCS measurements were carried out using a Zetasizer 3000 HS particle size analyser equipped with a 90° scattering and external fiber angle and a 632.8 nm helium–neon laser. Immediately prior to experiments, the samples were further diluted to a count rate of 100–300 Kcounts/s. Three runs containing 10 sub runs at 25 °C were performed to analyse the particle size distribution. Mono-modal analysis was chosen as analysis mode. All runs were checked for the polydispersity index (PI) (<0.25%), the merit (10–99%), the in range (>80%) and fit error (<0.005). For particle size characterization the mean intensity of each single run was used for calculating the mean average of the three runs in one measurement and the values for particle size were compared. Analysis of formulation API was performed.

2.2.5. AsFlFFF–MALS

The AsFlFFF system, consisting of a channel (connected to an Eclipse 2 separation system; Wyatt Technology Europe, Dernbach, Germany) and a HPLC pump (G1314A Iso Pump, Agilent Technologies, Santa Clara, CA, USA), was connected in series to a ternary detection system, combining an 18-angle static light-scattering detector (DAWN EOS, Wyatt Technology Corp., Santa Barbara, CA, USA), a variable wavelength UV–vis detector at a wavelength of 237 nm (G1314A VWD detector, 1100 series, Agilent Technologies) and differential refractive index (dRI) detector (Optilab rEX, Wyatt Technology Corp.). The AsFlFFF channel had a trapezoidal shape with a tip-to-top length of 26.5 cm and a broadness of 2.2 and 0.6 cm, respectively. The injection volume varied between 10 and 20 μl. A 250 μm thick Mylar spacer (Wyatt Technology) and a regenerated cellulose membrane with a cut off of 10 kDa as accumulation wall were employed. A typical AsFlFFF experiment consisted of three steps. First, relaxation of the sample was performed, followed by elution and finally rinsing of the channel. The applied method started with relaxation of the sample consisting of injection and focussing from minute 0 to 10. During this step, the carrier liquid entered the channel both from the outlet and inlet and concentrated the injected sample to a narrow band. The focusing step lasted for 5 min. Afterwards, over a period of 50 min, a channel flow rate of 1.0 ml/min and a cross flow rate of 0.7 ml/min were applied and the sample was transported towards the outlet. From minute 60 to 80 the system was flushed with the channel flow only. Unless mentioned otherwise, runs of different formulations were performed six times in a row and the channel was rinsed after each set of samples. The results from the last three runs were used for comparison. The system was controlled using Eclipse software Version 2.5 and data were analysed using ASTRA 5.3.2.15 (both Wyatt Technology). For graphical representation using GraphPad Prism 4.0 and Microsoft office excel 2007, the results of the Rayleigh ratio at 90°, UV absorbance and dRI detector were chosen. For analysis of the content of ritonavir and lopinavir in fractions of the carrier liquid leaving via the cross flow of each run was collected from minute 0 to 60. The carrier liquid from the channel flow was divided into fractions corresponding to characteristic signal changes in all three detectors. In order to saturate the membrane three runs were performed and during the fourth run fractions of the channel flow were collected. The cross flow of all four runs was collected. All experiments were done in triplicates.

Calculation of recovery (R) was performed relating the mass (μg) of each drug in each fraction or the cross flow collected during the entire fractionation to the total mass of injected drug (μg) as expressed in

$$R(\%) = \frac{mass_{fraction}}{mass_{total}} \times 100\%$$

The rms radius was calculated using the Berry method with a first-order polynomial fit in the particle mode. For calculation of

Table 1
Employed formulations for analysis using PSC and AsFlFFF.

Formulation	Lopinavir	Ritonavir	PVP/VA	Sorbitan monolaurate	Hydrophilic fumed silica
API	x	x	x	x	x
Placebo			x	x	x

the apparent molar mass the differential refractive index increment (dn/dc) was determined injecting six solutions of different concentrations of PVP/VA in the differential refractive index detector. The measured differential refractive index values were plotted against the concentrations of the PVP/VA solution. A dn/dc = 0.150 ml/g was derived from the slope. Calculation of the apparent weight average molar mass was performed applying the Debye method, second-order polynomial fit.

2.2.6. High performance liquid chromatography–mass spectrometry

20% acetonitrile and 1% formic acid were added to the collected fractions and each sample was analysed three times. D_3-testosterone was added as an external standard to all samples and standard solutions to a final concentration of 0.5 μg/ml. Lopinavir and ritonavir were separated on a 2695 Separation Unit (Waters, Milford, MA, USA) employing a Waters SunFire™ C18 column (1.0 mm × 50 mm, 2.5 μm particles). Isocratic elution with 50% of eluent A (99.9% purified water and 0.1% formic acid) and 50% of eluent B (90% acetonitrile, 9.9% purified water and 0.1% formic acid) was accomplished. The flow rate was 200 μl/min and the injection volume was 10 μl. Detection and quantification of the two drugs were performed on a Quattro-LC mass spectrometer (Micromass, Manchester, UK). The compounds were ionized applying positive electrospray ionization (ESI+) and the ions were introduced to the mass filters through a Z-spray source. The mass spectrometer was operated in the multiple reaction monitoring mode, and the following ion transitions (mass/charge ratio, m/z) were used for quantification: lopinavir (m/z 629.4 → m/z 183.0), ritonavir (m/z 721.1 → m/z 296.0) and testosterone-d_3 (m/z 292.2 → m/z 109.1) as external standard.

3. Results

Melt extrudates of both the API-containing and the placebo formulations appeared to be transparent. After dispersion in aqueous medium and agitation a turbid dispersion resulted in both cases. The solid state of the APIs was determined applying WAXS. The aqueous dispersions were investigated in terms of size and structures of assemblies. Methods of choice were PCS and AsFlFFF coupled to a MALS detector and offline quantification applying HPLC–MS/MS. Electron microscopic analysis of solid dispersion in aqueous media only showed unspecific, not distinctive assemblies (data not shown).

3.1. Wide angle X-ray scattering studies

The WAXS pattern showed no evidence of crystalline structures in the extrudate, which confirms the absence of crystalline lopinavir or ritonavir (data not shown). One can conclude that the extrudate was a true molecular dispersion of the APIs dissolved in the matrix.

3.2. Photon correlation spectroscopy

The particle size analysis using PCS for the API-containing formulation resulted in mono-modal distributions with an intensity-weighted mean particle size of 206.1 ± 16.6 nm (PI = 0.0703 ± 0.0437; n = 3). Mean particle size after 2, 3 and 4 h of stirring remained constant indicating that stirring time did not influence particle size (data not shown).

3.3. Asymmetrical flow field-flow fractionation

The fractograms of the two melt extrudate formulations, API and placebo (Fig. 2) showed characteristic patterns of peaks and shoulders within the signals from the three detectors coupled to the AsFlFFF system. Therefore, the fractograms were divided into sections related to occurrence of peaks and the two compositions were compared.

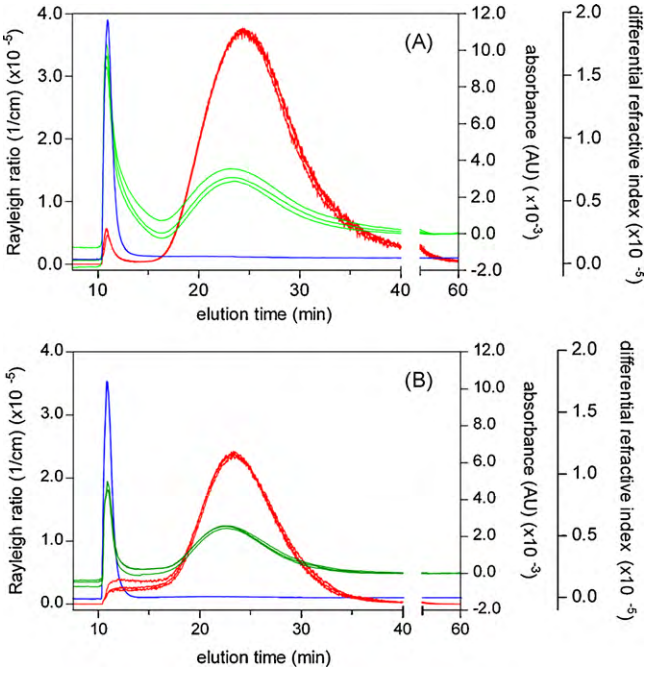

Fig. 2. Rayleigh ratio [1/cm] (red solid line), UV–vis absorbance [AU] (green solid line) and differential refractive index (blue solid line) of composition API (A) and placebo (B). (For interpretation of the references to color in this figure legend, the reader is referred to the web version of the article.)

3.3.1. Peak at approx. 10 min

When fractionating aqueous dispersion of the two formulations, all three detectors showed a peak right at the beginning of the elution process (at 10 min.). To clarify whether this peak represented an artefact from the pressure changes in the channel at the beginning of fractionation or a sample trace, the fractionation conditions were changed to a channel flow rate equal 1.0 ml/min and a cross flow gradient of 5.0 down to 0.5 ml/min over 40 min (Fig. 3). This change was expected to cause an enhanced retention of macromolecules or small particles (elution at later time) and a very strong retention of bigger particles. Under these conditions, as indicated by the dRI signal, the originally first peak was resolved into one

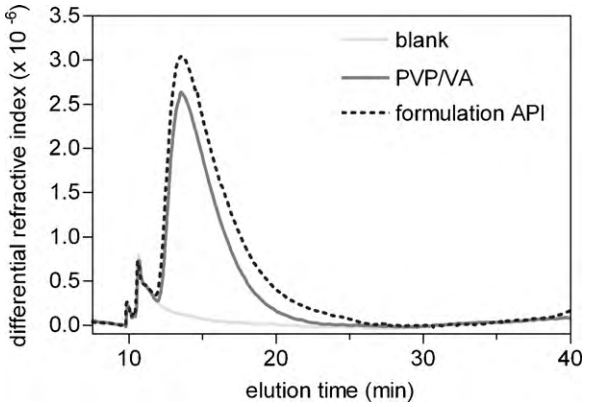

Fig. 3. Comparison of differential refractive index signal of PVP/VA solution, blank, and formulation API during elution mode applying a channel flow equal 1.0 ml/min and a cross flow gradient of 5.0–0.5 ml/min over 40 min.

Table 2
Detected amount (%) of lopinavir and ritonavir in channel flow and cross flow during the fourth run after injection of 20 μl of formulation API[a].

API	Channel flow	Cross flow
Lopinavir	62.9 (6.5)	152.5 (19.5)
Ritonavir	45.1 (5.7)	82.1 (5.0)

[a] Standard deviation is shown in parentheses.

major peak (around 15 min.), clearly separated from the injection peak. In the UV–vis detector and the MALS detector a signal was be observed as well but for reasons of clarity only the dRI signal is shown in Fig. 3. In order to get an idea of the nature of component eluting within the peak around 15 min, an AsFlFFF run with PVP/VA solution was employed under the exact same conditions. Comparison of the dRI signal of pure PVP/VA and the formulation API showed congruence.

3.3.2. Tail between 12 and 18 min (Fig. 2)

A tail was observable in the trace of the UV signal within the time frame of 12–18 min for the API composition but not for the placebo. The Rayleigh ratio signal was rather weak.

3.3.3. Peak between 20 and 40 min

The fractograms of the Rayleigh ratio of both formulations displayed a very strong peak. When looking at the UV signal of both formulations, a strong signal ran synchronic to the peak observed in the Rayleigh ratio and therefore, the signal was assumed to be caused by the same associates as those detected in the Rayleigh ratio.

3.3.4. Distribution of lopinavir and ritonavir

In order to get an idea whether and to which extent the APIs lopinavir and ritonavir were eluting in the channel flow during AsFlFFF, the fractogram of the API composition was divided into fractions (Fig. 4). The fractions were collected manually and analysed offline using HPLC–MS/MS. Considerable amounts of both APIs were recovered from the various channel flow-fractions. In fraction f1 lopinavir and ritonavir were present in marginal amounts only, the highest amounts of lopinavir and ritonavir were detected in fraction f2. The recovery of lopinavir was higher than that of ritonavir. In the subsequent fractions (f3–f5) ritonavir was evenly distributed in both formulations, while recovery of lopinavir decreased from fraction f2 to f4 and then stayed constant.

3.3.5. Recovery

Recovery in channel flow and cross flow of both APIs was calculated to evaluate potential interactions of the formulation with the ultra-filtration membrane serving as accumulation wall (Table 2). In preliminary experiments, the amount of APIs in the channel flow, cross flow and membrane of the third run after flushing was determined and it could be clearly seen that certain amount of APIs could be detected in the membrane fraction (data not shown). Comparing the amount of APIs in the fractions of the cross flow of the four runs in a row revealed an increase from the 1st to the 2nd run, slightly from the 2nd to the 3rd run and afterwards stayed rather constant (Fig. 5). Recoveries of both cross flow and channel flow of the fourth run in a row are given in Table 2. At this stage, lopinavir yielded higher recovery values, exceeding 100%.

3.3.6. Apparent molar mass and particle size

An apparent weight average molar mass of M_w = 570,000 g/mol was calculated for structures eluting during peak 1 (around minute 10). Calculation of the particle size distribution was performed for peak 2 (Fig. 6). The size of particles was dependent on presence of APIs.

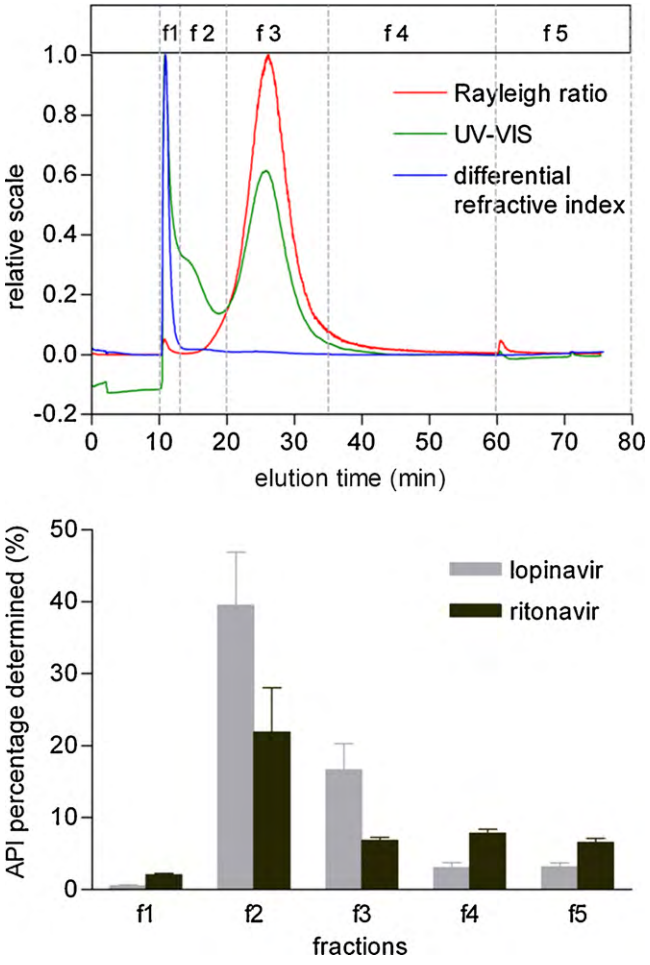

Fig. 4. Elution profile with fraction borders (top) for determination (amount in %) of lopinavir and ritonavir of composition API in fractions of channel flow (mean ± SD, n = 3). Collection was performed during the 4th run with an injection volume of 20 μl.

4. Discussion

Comparison of the fractograms of API-containing composition with a polymer solution indicated that the first peak at minute 10 consisted of colloidal polymer, mainly. Literature values of the molecular mass of PVP/VA range between 45,000 and 70,000 g/mol [21]. The calculated apparent molar mass found here was higher than reported for PVP/VA. Therefore, it may be assumed that assemblies eluting during this stage consisted not only of PVP/VA but also

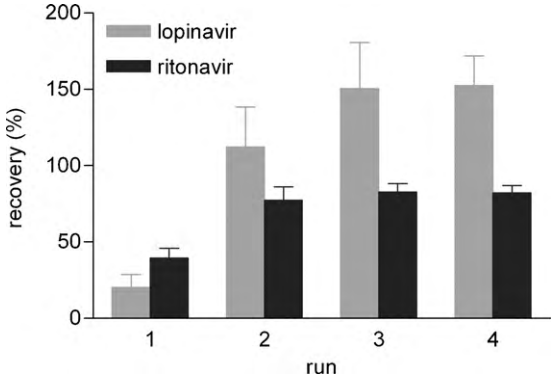

Fig. 5. Recovery (%) in the cross flow of lopinavir and ritonavir of four runs in a row injecting composition API (n = 3, mean ± SD).

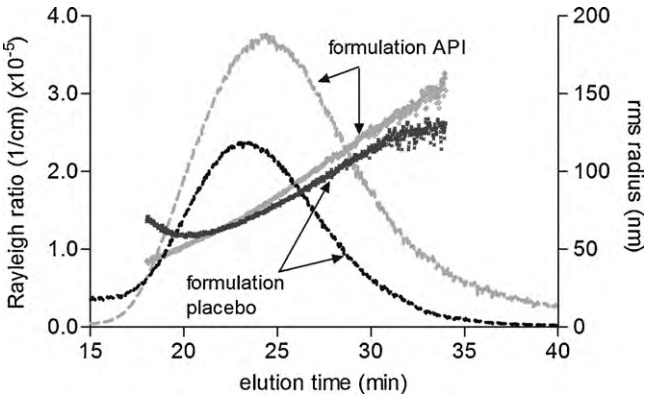

Fig. 6. Distribution of rms radius (nm) of formulation API and placebo and respective AsFlFFF–MALS fractograms.

of other compounds. Comparison of the API and the placebo fractograms regarding the tail in the trace of the UV signal between minute 12 and 18 revealed that both APIs were eluting to a significant extent with the channel flow at this time point. This assumption was confirmed by the quantitative analysis. More precisely the highest amount of both drugs was determined in fraction f2. A stable Rayleigh ratio signal could not be observed; therefore calculation of particle sizes was not possible. One reason could be that the particles were too small to be detected in the MALS detector and/or unstable for size analysis. Hence, it might be concluded that the APIs were present as supramolecular assemblies or very small particles. The detection of significant amounts of lopinavir and ritonavir in both, channel and cross flow indicated that the API was present partly in dissolved and in particulate form. The composition of the assembly responsible for the peak in the UV–vis signal and the Rayleigh ratio between minute 20 and 40 could not be clarified to full extent yet. API was obviously not the main cause for the occurrence of this peak because the peak was seen in the fractograms of both API- and placebo formulation. It is assumed that hydrophilic fumed silica and sorbitan monolaurate might elute at this time. On first instance the measured size did not appear to be in agreement with published primarily particle sizes of hydrophilic fumed silica of 7–16 nm [22] but formation of secondary agglomerates upon dispersion in aqueous media is described in literature [23]. The original concentration of the surfactant in the dispersion was 1.344 mg/ml. During experiment the sample was diluted up to a factor of 2500 and thus, the concentration should fall below the critical micelle concentration (cmc) ($cmc_{sorbitan\ monolaurate}$ = 0.05% (w/w)) [24]. Therefore, in the general understanding the surfactant should be present as monomer and thus be eluted via the cross flow. A recent PCS-study revealed sizes in the 40–70 nm magnitude irrespective whether dispersions of sorbitan monolaurate, hydrophilic fumed silica or melt extrudates containing sorbitan monolaurate and PVP/VA were investigated [13]. It remains to be clarified, if the surfactant was dissolved or if part of it was still existent in the structures eluting here.

It is unclear for the moment why the broad peak between minute 20 and 40 did not show up in the dRI fractograms. Hydrophilic fumed silica was present in a low concentration. One explanation could be that the concentration was too low for the dRI detector to be detected whereby the particles were big enough to change the Rayleigh ratio. Whether the amounts of APIs found in this fraction were associated with the assemblies or represent carryover from the previous fraction could not be decided on the information available so far. The particle size analysis points towards that certain amount of API was connected to the assemblies eluting during this peak because presence of API had an effect on size.

Taken the recovery of both APIs in cross flow and channel flow into account it can be concluded that the APIs were not completely dissolved at the time of separation but rather were existent in fine particles. For the increase of recovery in four runs in a row, following explanations may be given (1) drug particles were pressed into pores of the accumulation wall or (2) API adsorbed to the membrane during the first run. On the one hand adsorption of particles on the membrane may change interactions between membrane and particles. On the other hand loss of particles falsifies the results of the fractionation. During the second run drug may be dissolved from these retained particles or adsorbed drug washed off and therefore, the amount in the cross flow increased. Furthermore, pores of the membrane were saturated with drug particles and logically, more particles were able to be eluted. Differences in the shape of the peak during elution could not be observed but only variability in the height of the peak.

Applying AsFlFFF gives the opportunity to distinguish between several assemblies formed during dissolution and is regarded as a valuable new tool for investigation of melt extrudates regarding in situ nanoparticle formation. Furthermore, the technique may give information about the stability of nanoparticles containing drugs and their dissolution behaviour. Comparison of size analysis applying PCS and AsFlFFF demonstrated that using AsFlFFF provided a more detailed insight into size distribution.

However, one has to bear in mind that sodium nitrate represents a rather simple medium. It is well suited for the use as carrier liquid in flow field-flow fractionation. Furthermore, during the relaxation step the sample got concentrated whereas it was diluted to a high degree during the experiments. To which extent this environmental change had an influence on particle formation needs to undergo further investigations.

5. Conclusions

Analysis of solid dispersions as melt extrudates (e.g. Meltrex® formulations) in aqueous media by AsFlFFF revealed that even after extensive dilution most likely several different types of supramolecular or nanoparticulate structures in aqueous dispersion of melt extrudate formulations were existent: colloidal polymer, nanoparticulate aggregates of hydrophilic fumed silica and/or surfactant, and supramolecular (nanoparticulate) assemblies of API. The third major fraction containing hydrophilic fumed silica and/or the lipophilic surfactant sorbitan monolaurate appeared to contain non-negligible amounts of API as well, but clear distinction between carryover of the drug and drug incorporated in or adsorbed to the surfactant/hydrophilic fumed silica assembly was not possible. Furthermore, particle structures, which represent combinations of two or more components of the formulation, may have been formed.

In summary, it may be concluded that the drugs lopinavir and ritonavir from this particular solid dispersion system were in situ released as nanoparticles. Such nanoparticles are expected to show fast dissolution rates as consequence of their small particle sizes. It remains to be elucidated how far the findings reported here hold true for other melt extrudate formulations. Further investigations are currently carried out in our laboratories.

Acknowledgements

This study was supported by SOLIQS, Abbott GmbH and Co. KG, Ludwigshafen, Germany. We would like to thank Dr. Ulrich Westedt, Dr. Bernd Liepold and Dr. Joerg Rosenberg for their contribution to discussions.

References

[1] C.A. Lipinski, F. Lombardo, B.W. Dominy, P.J. Feeney, Experimental and computational approaches to estimate solubility and permeability in drug discovery and development settings, Adv. Drug Deliv. Rev. 23 (1997) 3–25.

[2] W.L. Chiou, S. Riegelman, Pharmaceutical applications of solid dispersion systems, J. Pharm. Sci. 60 (1971) 1281–1302.

[3] D.A. Miller, J.W. McGinity, R.O. Williams, in: R.O. Williams, R.D. Taft, J.T. McConville (Eds.), Advanced Drug Formulation Design to Optimize Therapeutic Outcomes, Taylor and Francis, New York, 2008, pp. 451–491.

[4] J. Breitenbach, Melt extrusion: from process to drug delivery technology, Eur. J. Pharm. Biopharm. 54 (2002) 107–117.

[5] D. Law, E.A. Schmitt, K.C. Marsh, E.A. Everitt, W. Wang, J.J. Fort, S.L. Krill, Y. Qiu, Ritonavir-PEG 8000 amorphous solid dispersions: in vitro and in vivo evaluations, J. Pharm. Sci. 93 (2004) 563–570.

[6] D.J. Kempf, K.C. Marsh, G. Kumar, A.D. Rodrigues, J.F. Denissen, E. McDonald, M.J. Kukulka, A. Hsu, G.R. Granneman, P.A. Baroldi, E. Sun, D. Pizzuti, J.J. Plattner, D.W. Norbeck, J.M. Leonard, Pharmacokinetic enhancement of inhibitors of the human immunodeficiency virus protease by coadministration with ritonavir, Antimicrob. Agents Chemother. 41 (1997) 654–660.

[7] H.L. Sham, D.J. Kempf, A. Molla, K.C. Marsh, G.N. Kumar, C.M. Chen, W. Kati, K. Stewart, R. Lal, A. Hsu, D. Betebenner, M. Korneyeva, S. Vasavanonda, E. McDonald, A. Saldivar, N. Wideburg, X. Chen, P. Niu, C. Park, V. Jayanti, B. Grabowski, G.R. Granneman, E. Sun, A.J. Japour, J.M. Leonard, J.J. Plattner, D.W. Norbeck, ABT-378, a highly potent inhibitor of the human immunodeficiency virus protease, Antimicrob. Agents Chemother. 42 (1998) 3218–3224.

[8] C.E. Klein, Y.L. Chiu, W. Awni, T. Zhu, R.S. Heuser, T. Doan, J. Breitenbach, J.B. Morris, S.C. Brun, G.J. Hanna, The tablet formulation of lopinavir/ritonavir provides similar bioavailability to the soft-gelatin capsule formulation with less pharmacokinetic variability and diminished food effect, J. Acquir. Immune. Defic. Syndr. 44 (2007) 401–410.

[9] C. Leuner, J. Dressman, Improving drug solubility for oral delivery using solid dispersions, Eur. J. Pharm. Biopharm. 50 (2000) 47–60.

[10] E. Karavas, E. Georgarakis, M.P. Sigalas, K. Avgoustakis, D. Bikiaris, Investigation of the release mechanism of a sparingly water-soluble drug from solid dispersions in hydrophilic carriers based on physical state of drug, particle size distribution and drug–polymer interactions, Eur. J. Pharm. Biopharm. 66 (2007) 334–347.

[11] J. Albers, R. Alles, K. Matthee, K. Knop, J.S. Nahrup, P. Kleinebudde, Mechanism of drug release from polymethacrylate-based extrudates and milled strands prepared by hot-melt extrusion, Eur. J. Pharm. Biopharm. 71 (2009) 387–394.

[12] D.Q.M. Craig, The mechanisms of drug release from solid dispersions in water-soluble polymers, Int. J. Pharm. 231 (2002) 131–144.

[13] I. Tho, B. Liepold, J. Rosenberg, M. Maegerlein, M. Brandl, G. Fricker, Formation of nano/micro dispersions with improved dissolution properties upon dispersion of ritonavir melt extrudate in aqueous media, Eur. J. Pharm. Sci. (2010), doi:10.1016/j.ejps.2010.02.003.

[14] W. Fraunhofer, G. Winter, The use of asymmetrical flow field-flow fractionation in pharmaceutics and biopharmaceutics, Eur. J. Pharm. Biopharm. 58 (2004) 369–383.

[15] J.C. Giddings, Field-flow fractionation—analysis of macromolecular, colloidal, and particulate materials, Science 260 (1993) 1456–1465.

[16] M Andersson, B. Wittgren, K.G. Wahlund, Accuracy in multiangle light scattering measurements for molar mass and radius estimations. Model calculations and experiments, Anal. Chem. 75 (2003) 4279–4291.

[17] S. Hupfeld, D. Ausbacher, M. Brandl, Asymmetrical flow field flow fractionation of liposomes: optimization of fractionation variables, J. Sep. Sci. 32 (2009) 1465–1470.

[18] S. Hupfeld, H.H. Moen, D. Ausbacher, H. Hass, M. Brandl, Liposome fractionation and size analysis by asymmetrical flow field-flow fractionation/multi-angle light scattering: influence of ionic strength and osmotic pressure of the carrier liquid, Chem. Phys. Lipids 163 (2010) 141–147.

[19] A. Litzen, K.G. Wahlund, Effects of temperature, carrier composition and sample load in asymmetrical flow field-flow fractionation, J. Chromatogr. 548 (1991) 393–406.

[20] M.H. Moon, I. Park, Y.H. Kim, Size characterization of liposomes by flow field-flow fractionation and photon correlation spectroscopy—effect of ionic strength and pH of carrier solutions, J. Chromatogr. A 813 (1998) 91–100.

[21] V. Bühler, in: V. Bühler (Ed.), Polyvinylpyrrolidone Excipients for Pharmaceuticals, Springer, Berlin, 2005, pp. 179–219.

[22] S.C. Owen, in: R.C. Rowe, P.L. Sheskey, S.C. Owen (Eds.), The Handbook of Pharmaceutical Excipients, Pharmaceutical Press, London, 2006, pp. 188–191.

[23] H. Barthel, Surface interactions of dimethylsiloxy group-modified fumed silica, Colloids Surf. A 101 (1995) 217–226.

[24] S.Y.D. Lin, J.M. Krochta, Whey protein coating efficiency on surfactant-modified hydrophobic surfaces, J. Agric. Food Chem. 53 (2005) 5018–5023.